Digital - domain embedding method for groundwater flow at the industrial waste landfill on Teshima Island

Takako Yoshii[1] and Hideyuki Koshigoe[2]

[1] Graduate School of Engineering, Chiba University, Japan,
[2] Department of Urban Environment Systems, Chiba University, Japan **

Abstract. In this article we propose a numerical method to simulate the groundwater flow at the industrial waste landfill on Teshima Island. The solution method combines finite difference method, digital color image and domain embedding method. Domain embedding method is also called fictitious domain method. The digital color image consists of so many pixels and each of which forms a small square, is addressable and has the color intensity of RGB. Getting these informations from the digital image, we introduce the notion of cell which is a set of pixels, and approximate the domain of industrial wastes and soil layers by these cells. We call it the generation of regular cells. We then construct the finite difference method on cells and show numerical simulations for the groundwater flow.

1 Introduction

The purpose of this article is to establish a new finite difference method coupled with digital color image and to show the groundwater flow through industrial wastes and soil layers. The characteristic is that the digital color image and the domain embedding method developed from Lions ([6]) play an important role.
We first state the background of the landfill on Teshima Island and the data by the borehole logging([8]). From 1978 to 1990, the large-scale industrial wastes were illegally dumped to a part of Teshima Island in Japan. The area, the weight and the height of the industrial waste heaped on Teshima Island are about 7 ha, 500,000 tonnes and 16 m, respectively. The environmental report showed that groundwater in the alluvium and granite layers were contaminated at levels above the environmental water criteria and the contaminated groundwater was leaching to the Seto Inland Sea from the dumping site of Teshima Island ([8],[9]). Therefore it is important to predict the groundwater flow by the numerical simulation using the data of the borehole logging.
We now introduce the data of the borehole logging from the investigation result of MIC ([8]).

** Corresponding author: H.Koshigoe, E-mail Address: koshigoe@tu.chiba-u.ac.jp
This work was partially supported by JSPS KAKENHI (22540113).

Drilling points and distribution of wastes in the landfill site
The drilling survey was carried out in 1995 ([8]). Fig.1.1 shows its drilling points and distribution of wastes in the landfill site on Teshima Island. The upside in Fig.1.1 is the Seto Inland Sea. The interest of this paper is to show the groundwater flow along the geological profile of F-line, which is marked by the letter F below.

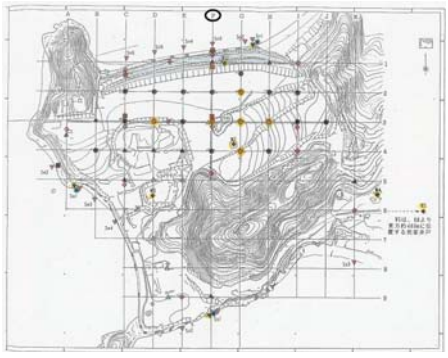

Fig. 1. Drilling points(・) on the area of damping site

Geological profile of F-line and piezometric head
Fig.2 shows the geological profile of F-line which were reported by the above drilling survey([8]). This geological profile consists of shredderdust(Ω_1), cinder(Ω_3), sandy soil(Ω_2), fresh granite(Ω_4), and fractured granite(Ω_5). And the areas of Ω_1 and Ω_3 are occupied by the materials of industrial wastes.

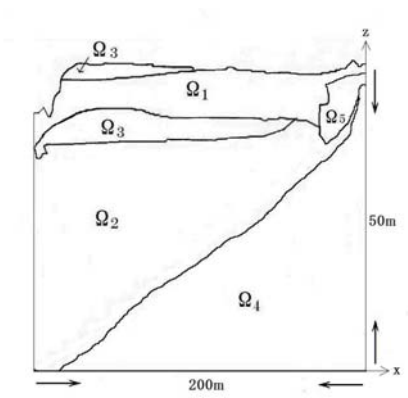

Fig. 2. Geological profile of F-line (X: the horizontal, Z: the vertical)

The notion of the piezometric head is expressed as the groundwater flow potential according to the Bernoulli principle and the piezometric heads had been investigated at two points on the geological profile of F-line, where are 100 m and 200 m from the Seto Inland Sea([8]).

Characteristics of numerical method in this article
Each layer of the geological profile is the complex shape as the above Fig.2. But using the digital color image, we note that it is possible to approximate each layer of the geological profile by pixels, each of which is a picture element of the digital color image. Hence the numerical method we shall propose here is that we first convert the geological profile (Fig.2) into a digital color image (Fig.3) below and that we construct the finite difference method by use of pixels.

Fig. 3. Digital color image for the geological profile

The content of this paper is as follows.
In Section 2, we shall state a mathematical model of the groundwater flow and its fictitious domain formulation which are based on the data of the drilling survey ([8]). In Section 3, the above fictitious domain will be digitized and we propose a numerical formulation by use of the digital color image. In Section 4, we shall present the numerical simulation of the groundwater flow through the geological profile and compare the numerical result with the data of the drilling survey. This section is our conclusion. However the huge earthquake of M 9.0 occurred on 11 March 2011 in Japan's Tohoku region. In order to prevent high level radioactivity contaminated water which flows from the first nuclear power plant of Fukushima into the Pacific Ocean, it is necessary to built the impermeable wall on the sea side within two years. Hence in the additional section 5, we show that the digital-embedding method is also effective to calculate and predict the groundwater flow in the case where there is the impermeable wall on the sea side.

2 A mathematical model based on the drilling survey

2.1 Groundwater flow in general

Before proceeding to the mathematical model based on the drilling survey, we state the piezometric head, the Darcy's law and the governing equation of a groundwater flow, which are known in the field of groundwater hydraulics ([5]).

(A) The position of a piezometric head is given by a sum of an elevation and pressure head as follows:

$$u = z + \frac{p}{\rho g} \tag{1}$$

where z is the vertical distance, p is the pressure, ρ is the fluid density and g is the acceleration of gravity. Hence the unit of the piezometric head is meter[m].
(B) The Darcy's law is defined by

$$\boldsymbol{v}_s = -k\nabla u \tag{2}$$

where $\boldsymbol{v}_s$ is called the Darcy's velocity and it is described by the permeability k and the hydraulic gradient ∇u.
(C) The governing equation of a groundwater flow has a form

$$S_0 \frac{\partial u}{\partial t} = -\nabla \cdot \boldsymbol{v}_s \tag{3}$$

where S_0 is a specific storage.
Therefore the following equation (4) is derived from the equation (2) and (3)

$$S_0 \frac{\partial u}{\partial t} = \mathrm{div}(k\nabla u). \tag{4}$$

2.2 Data of drilling survey at Teshima landfill

In this paper we consider a steady state flow in (4) since the velocity of infiltration in Teshima is 1 mm/day and slow ([8]). Therefore, we get a basic governing equation of the steady groundwater flow from (1)-(4);

$$\mathrm{div}(k\nabla u) = 0. \tag{5}$$

Remark 1. The permeability(k) is ability of material to allow water to move through it, expressed in terms of [cm/s]. In this article we use the permeability and the geological profile as shown in Table 1 and Figure 4, respectively ([8]).

Table 1. Permeability of earth materials and notations

material	notation of layer	permeability[cm/s]	notation of permeability
shredderdust	Ω_1	6.72×10^{-4}	k_1
cinder	Ω_3	1.30×10^{-6}	k_3
sandy soil	Ω_2	1.22×10^{-3}	k_2
fresh granite	Ω_4	5.31×10^{-5}	k_4
fractured granite	Ω_5	2.23×10^{-3}	k_5

And we also use the piezometric head(u) by the drilling survey along F-line ([8]):

$$u = 10.7 \text{ m on } \Gamma_2$$
$$u = 3.11 \text{ m at the point } \diamond.$$

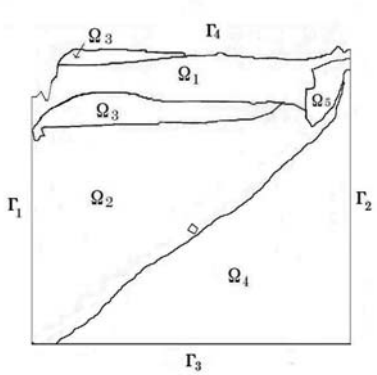

Fig. 4. Layer (Ω_i) and boundary (Γ_i)

2.3 Mathematical model based on the drilling survey

Now let's show the mathematical model of the groundwater flow at Teshima landfill. Using the geological profile (cf. Fig.4) and its permeability $\{k_i\}$ (cf. Table 1), we define the function $k(x, z)$ as follows.

$$k(x,z) = \sum_{i=1}^{5} k_i \ \chi_{\Omega_i}(x,z)$$

where

$$\chi_{\Omega_i}(x,y) = \begin{cases} 1 & \text{if } (x,y) \in \Omega_i \quad (i = 1,2,3,4,5), \\ 0 & \text{otherwise.} \end{cases}$$

Then the following mathematical model is deduced from (5).

Mathematical model

Find $u \in H^1(\Omega)$ satisfying

$$\begin{cases} \mathrm{div}(\, k(x,z)\nabla u) = 0 \quad \text{in } D'(\Omega), \\ u = 0 \quad \text{on } \ \Gamma_1, \quad u = g_2 \quad \text{on } \Gamma_2, \\ k\frac{\partial u}{\partial n} = 0 \ \text{ on } \ \Gamma_3, \ \ k\frac{\partial u}{\partial n} = 0 \quad \text{on } \Gamma_4. \end{cases}$$

Here $D'(\Omega)$ means the Schwarz distribution and g_2 is the piezometric head. Here g_2 is the datum investigated by the borehole logging ([8]). $\Omega = \Omega_1 \cup \Omega_2 \cup \Omega_3 \cup \Omega_4 \cup \Omega_5$ and n is the outer normal vector.

Remark 2. It follows from the mathematical model that

$$[\ k\ \frac{\partial u}{\partial n}\ ] = 0 \tag{6}$$

where [ ] denotes the jump on geologic boundary surfaces.

In fact, denoting u_i the piezometric head in each layer Ω_i, $\delta_{\Gamma_{i,j}}$ Dirac Delta

function on $\Gamma_{i,j}$ $(= \partial\bar{\Omega}_i \cap \partial\bar{\Omega}_j)$ and n is the outer normal vector on $\Gamma_{i,j}$, the Schwarz distribution shows that

$$\begin{aligned}\mathrm{div}\big(\, k(x,z)\nabla u\big) &= \sum_{i,j=1}^{5} \big(k_i\, \frac{\partial u_i}{\partial n} - k_j\, \frac{\partial u_j}{\partial n}\big)\delta_{\Gamma_{i,j}} + k(x,z)\Delta u \\ &= 0 \qquad\qquad \text{in } D'(\Omega).\end{aligned}$$

Hence we get (6), i.e.,

$$k_i\, \frac{\partial u_i}{\partial n} = k_j\, \frac{\partial u_j}{\partial n} \quad \text{on } \Gamma_{i,j}.$$

Therefore the mathematical model is also rewritten as follows:

Find $u_i \in H^1(\Omega_i)$ $(i = 1,2,3,4,5)$ satisfying

$$\begin{aligned}
\Delta u_i &= 0 && \text{in } \Omega_i \ \ (\, i = 1,2,3,4,5\,), \\
u_i &= u_j && \text{on } \partial\bar{\Omega}_i \cap \partial\bar{\Omega}_j \ \ (\, i \neq j\,), && (7)\\
k_i\frac{\partial u_i}{\partial n} &= k_j\frac{\partial u_j}{\partial n} && \text{on } \partial\bar{\Omega}_i \cap \partial\bar{\Omega}_j \ \ (\, i \neq j\,), && (8)\\
u_i &= 0 && \text{on } \Gamma_1 \ \ (\, i = 1,2,3\,), \\
u_i &= g_2 && \text{on } \Gamma_2 \ \ (\, i = 1,4,5\,), \\
k_i\frac{\partial u_i}{\partial n} &= 0 && \text{on } \Gamma_3 \ \ (\, i = 4\,), \\
k_i\frac{\partial u_i}{\partial n} &= 0 && \text{on } \Gamma_4 \ \ (\, i = 1,3\,).
\end{aligned}$$

Remark 3. The equations (7) and (8) on geologic boundary surfaces are a type of transmission conditions which was introduced by Lions ([2],[6]).

3 Computational method by use of digital color image

In this section, we present a numerical model coupled with a digital color image for the mathematical model and our computational method which combines the regular mesh in finite difference approximations with pixels of the digital image ([7], [10]).

3.1 Digital approximation of geological profile by pixels

The digital color is composed of pixel which are arranged in two dimensional grid. Each pixel is addressable and has a color intensities. Using the about fact, we convert the geological profile (Fig.3) into a digital color image (Fig.5) below. In this digital image based on the geological layers, color is assigned to each pixel as shown in Fig.5. In the obtained color image, it is noted that aspect ratio of the geological profile,1 width : 1 height, is changed into 2,000 pixel width : 500 pixel height.

Fig. 5. Six color image (2000 pixels × 500 pixels)

Table 2. Color corresponding to layer

layer	notation	color of layer
shredderdust	Ω_1	blue
cinder	Ω_3	purple
sandy soil	Ω_2	turquoise
fresh granite	Ω_4	green
fractured granite	Ω_5	yellow
air	Ω_6	white

We now introduce a important notice which we call regular cells to compute the mathmatical model in three steps.

Step 1: RGB value (Rp, Gp, Bp) at each pixel

A digital color image pixel is just a RGB data value. Each pixel's color sample has three numerical RGB components (Red, Green, Blue) to represent the color. These three RGB components are three 8-bit numbers for each pixel (p). We denote it by (Rp, Gp, Bp).

Step 2: Cell value (Rc, Gc, Bc) at each cell

In our computation, we define a cell which forms N_c pixels width and N_c pixels height. Each cell consists of $N_c \times N_c$ pixels.
Using the RGB value (Rp, Gp, Bp) of each pixel (p), we define the cell value (Rc, Gc, Bc) at each cell as follows:

Rc = the average of Rp values of pixels included in a cell,
Gc = the average of Gp values of pixels included in a cell,
Bc = the average of Bp values of pixels included in a cell.

Step 3: The generation of regular cells

Calculating the cell values of Fig.5, we introduce regular cell $\{\widetilde{\Omega}_i\}$ of $\{\Omega_i\}$ by as follows.

$$\begin{aligned}
\widetilde{\Omega}_1 &= \{ \text{ cells; cell value } = \ (\ 0\ \ , 0\ \ , 255\ ) \ \}, \\
\widetilde{\Omega}_2 &= \{ \text{ cells; cell value } = \ (\ 0\ \ , 255\ , 255\ ) \ \}, \\
\widetilde{\Omega}_3 &= \{ \text{ cells; cell value } = \ (\ 255\ , 0\ \ , 255\ ) \ \}, \\
\widetilde{\Omega}_4 &= \{ \text{ cells; cell value } = \ (\ 0\ \ , 255\ , 0\ \ ) \ \}, \\
\widetilde{\Omega}_5 &= \{ \text{ cells; cell value } = \ (\ 255\ , 255\ , 0\ \ ) \ \}, \\
\widetilde{\Omega}_6 &= \{ \text{ cells; cell value } = \ (\ 255\ , 255\ , 255\ ) \ \}.
\end{aligned}$$

Here we let the cell of geologic boundary surfaces belong to its lower layer.

3.2 Numerical formulation for the mathematical model

In the previous section, we introduced the regular cells. Then let $D = \widetilde{\Omega}_1 \cup \widetilde{\Omega}_2 \cup \widetilde{\Omega}_3 \cup \widetilde{\Omega}_4 \cup \widetilde{\Omega}_5 \cup \widetilde{\Omega}_6$.

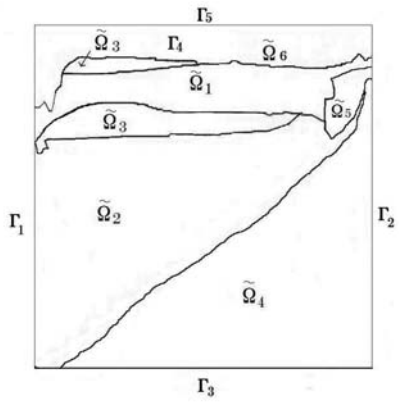

Fig. 6. Digital fictitious domain

Using the regular cell $\widetilde{\Omega}_i$, we define a function $\widetilde{k}(x,z)$ such that

$$\widetilde{k}(x,z) = \sum_{i=1}^{6} k_i \ \chi_{\widetilde{\Omega}_i}(x,z) \tag{9}$$

where $\{\ k_1, k_2, k_3, k_4, k_5\ \}$ is the permeability and k_6 is a parameter in $\widetilde{\Omega}_6$, which is the domain occupied with air. We now propose the following numerical formulation for the mathematical model.

Numerical formulation for the mathematical model

Find $u \in H^1(D)$ satisfying

$$\begin{cases} \mathrm{div}(\widetilde{k}(x,z)\nabla u) = 0 \quad \text{in } D'(D) \\ u = 0 \quad \text{on } \ \Gamma_1, \quad u = g_2 \quad \text{on } \Gamma_2 \cap \bar{\Omega}_2 \\ k\frac{\partial u}{\partial n} = 0 \ \text{ on } \ \Gamma_3, \ \ k\frac{\partial u}{\partial n} = 0 \quad \text{on } \Gamma_5. \end{cases}$$

Remark 4. From the viewpoint of Lions ([2],[6]), Fujita ([1]) and Kawarada([1],[3]), we approximate the Neumann's condition on Γ_4 in the mathematical model by choosing k_6 as a sufficiently small number in this formulation.

4 Numerical computation

The numerical computation for this formulation is based on a kind of finite difference approximations defined on "cells". The size of the regular cell corresponds to the width of N_c pixels.

4.1 Data in Numerical formulation

The piezometric head g_2 [m] on Γ_2 and the permeability k_i [m/s] $(i = 1, 2, 3, 4, 5)$ in the numerical formulation are given as follows [8].

$g_2 = 10.7$ m ,

$k_1 = 6.72 \times 10^{-6}$ m/s , $k_2 = 12.2 \times 10^{-6}$ m/s , $k_3 = 0.013 \times 10^{-6}$ m/s, $k_4 = 0.531 \times 10^{-6}$ m/s, $k_5 = 22.3 \times 10^{-6}$ m/s .

From Remark 4, we choose the parameter k_6 such that

$k_6 = 1.0 \times 10^{-9}$ m/s.

4.2 Finite difference scheme on cells $\diamond_{i.j}$

We first define

N_c=2,

h = the width of N_c pixels, which means the width of cell,

$\widetilde{k}_{i,j}$ = the permeability of cell $\diamond_{i.j}$ on D which is defined by (9), and

$u_{i,j}$ = the numerical value on cell $\diamond_{i.j}$ in D.

Then the numerical problem is to find $u_{i,j}$ on cell $\diamond_{i.j}$ satisfying

$$\begin{aligned} &\frac{1}{h}\Big(\frac{\widetilde{k}_{i+1,j}+\widetilde{k}_{i,j}}{2}\ \frac{u_{i+1,j}-u_{i,j}}{h} - \frac{\widetilde{k}_{i,j}+\widetilde{k}_{i-1,j}}{2}\ \frac{u_{i,j}-u_{i-1,j}}{h}\Big) \\ &+\frac{1}{h}\Big(\frac{\widetilde{k}_{i,j+1}+\widetilde{k}_{i,j}}{2}\ \frac{u_{i,j+1}-u_{i,j}}{h} - \frac{\widetilde{k}_{i,j}+\widetilde{k}_{i,j-1}}{2}\ \frac{u_{i,j}-u_{i,j-1}}{h}\Big) = 0 \end{aligned} \tag{10}$$

$+$ Boundary conditions.

4.3 The result of numerical simulation

From the finite difference scheme (10) on cells, we get numerical solution u_h, calculate velocity of the groundwater flow by use of the Darcy's law (2), and draw the groundwater flow by our programming with OpenGL. Then the groungwater flow is as follows. The maximum value and the minimum value of the velocity vector designated in red and in blue in Fig. 7 are 4.35×10^{-4} m/s and 1.17×10^{-8} m/s, respectively.

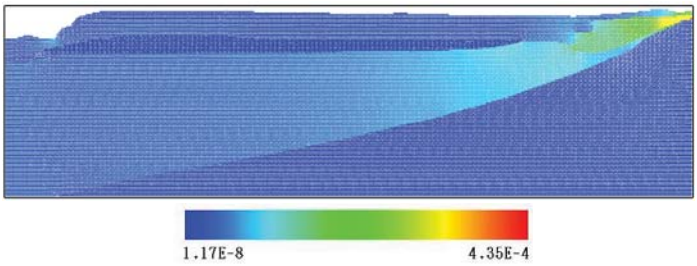

Fig. 7. Direction and strength of groundwater flow

In order to describe clearly the vector of the flow, we show a result of the numerical computation in the case where Nc=10 (see Fig.8).

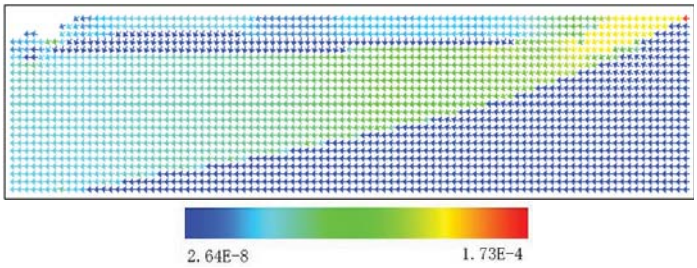

Fig. 8. Vector of groundwater flow

From the above results of the numerical simulations, the groundwater flows slowly through the shredder dust in the industrial waste layer, the sandy soil and fractured granite in soil layers. And this groundwater also flows to the direction of the Seto Inland Sea.

Since having the value of the piezometric heads in all domain by the above calculation, we now compare this result with another datum ([8]) of the piezometric head investigated by the borehole logging at the point ⋄ in Fig.9 below.

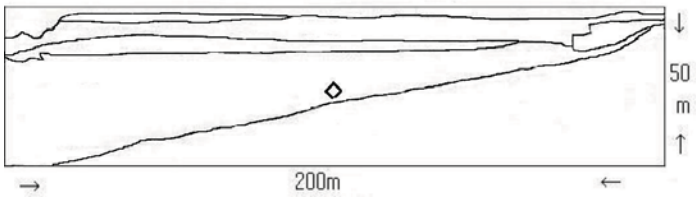

Fig. 9. Another borehole logging point ⋄.

At the point $\diamond$ where is 100 m from sea side and 22 m from top of the shredderdust, the piezometric heads by the borehole logging and the numerical result are 3.11 m and 3.17 m, respectively. Therefore this numerical method proposed here is useful to presume the groundwater flow at the industrial waste landfill.

5 Additional section

Earthquake in Japan's Tohoku region occurred on Friday, 11 March 2011. In order to prevent that high level radioactivity contaminated water flows from the first nuclear power plant of Fukushima into the Pacific Ocean, Tepco started building the impermeable wall on the sea side. Hence we now show additional numerical simulations of groundwater flow in the case where there is the impermeable wall on the sea side from the view point of our numerical method.

5.1 Numerical model with impermeable wall

Let Ω_7 be the domain of the impermeable wall and we generate the regular cells by our developed program. Then let $D = \widetilde{\Omega}_1 \cup \widetilde{\Omega}_2 \cup \widetilde{\Omega}_3 \cup \widetilde{\Omega}_4 \cup \widetilde{\Omega}_5 \cup \widetilde{\Omega}_6 \cup \widetilde{\Omega}_7$. And we introduce a sufficient small parameter k_7 on $\widetilde{\Omega}_7$ as well as k_6 on $\widetilde{\Omega}_6$.

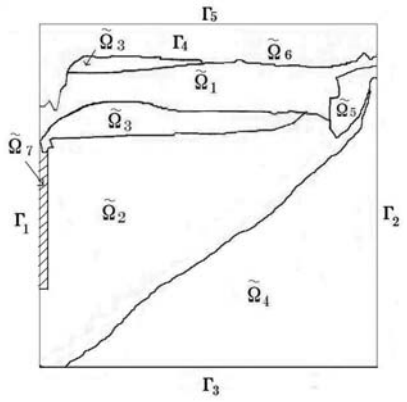

Fig. 10. Digital fictitious domain

Using the regular cell $\widetilde{\Omega}_i$(i=1,2,3,4,5,6,7), we define a function $\widetilde{k}(x,z)$ such that

$$\widetilde{k}(x,z) = \sum_{i=1}^{7} k_i \ \chi_{\widetilde{\Omega}_i}(x,z) \tag{11}$$

Then our numerical model is as follows.

Numerical model

Find $u \in H^1(D)$ satisfying

$$\begin{cases} \operatorname{div}(\widetilde{k}(x,z)\nabla u) = 0 \quad \text{in } D'(D) \\ u = 0 \quad \text{on } \Gamma_1, \quad u = g_2 \quad \text{on } \Gamma_2 \\ k\frac{\partial u}{\partial n} = 0 \text{ on } \Gamma_3, \quad k\frac{\partial u}{\partial n} = 0 \quad \text{on } \Gamma_5, \\ k\frac{\partial u}{\partial n} = 0 \quad \text{on } \partial\widetilde{\Omega}_2 \cap \partial\widetilde{\Omega}_7. \end{cases}$$

The following numerical results correspont to the cases where there are the impermiable walls builted on 10 meter, 20 meter, 30 meter deep below sealevel. And the numerical simulations show the flows of groundwater and their velocities around the impermeable walls.

[10 meter deep below sea level]

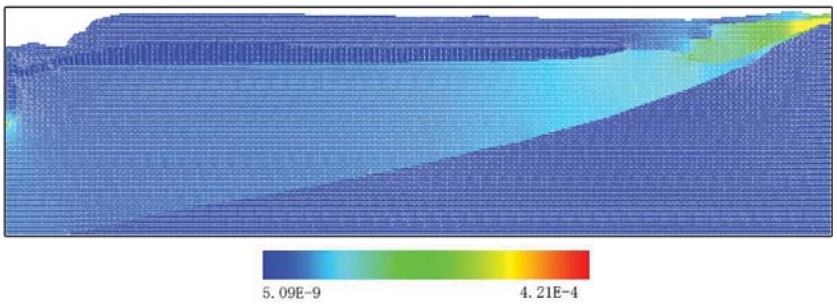

Fig. 11. Nc=2: Direction and strength of groundwater flow.

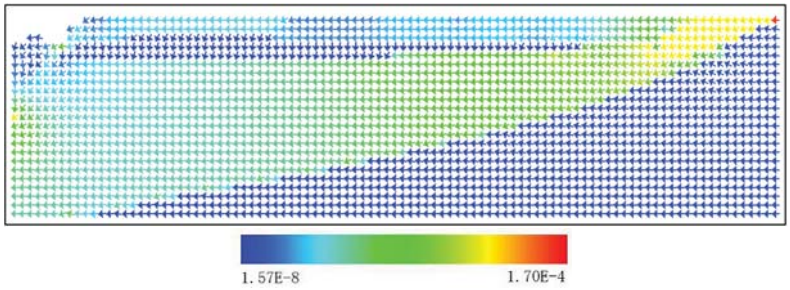

Fig. 12. Nc=10: Vector of groundwater flow.

[20 meter deep below sea level]

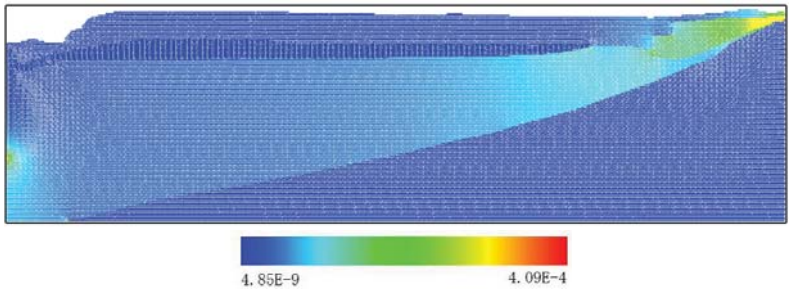

Fig. 13. Nc=2: Direction and strength of groundwater flow.

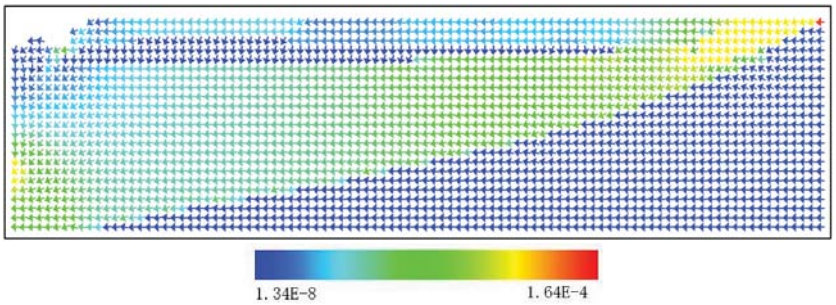

Fig. 14. Nc=10: Vector of groundwater flow.

[30 meter deep below sea level]

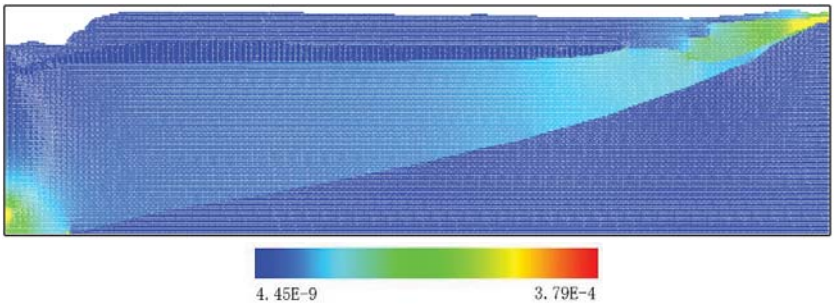

Fig. 15. Nc=2: Direction and strength of groundwater flow.

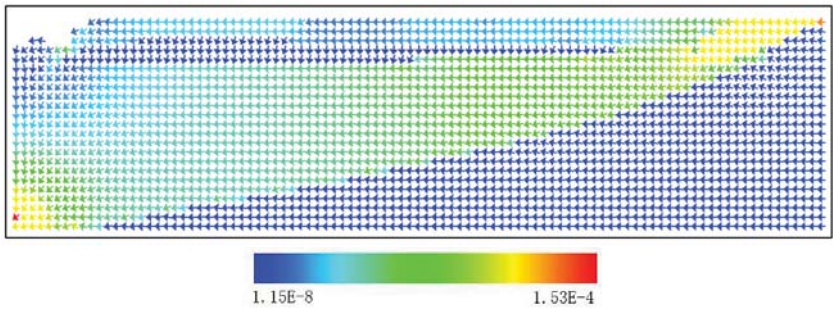

Fig. 16. Nc=10: Vector of groundwater flow.

6 Conclusion

In this paper, we proposed the new finite difference method using the digital color image and fictitious domain method, and showed the groundwater flow through the industrial waste and layers. And calculating the groundwater flow, we first convert the geological profile into the digital color image and then develop the following program.

(C1) The program which generates the regular cell from 24 bit bmp file,
(C2) The program of the finite difference method defined on the regular cells in stead of the grid points,
(C3) The visualization program which expresses the flow by the vector and color.

We now conclude that the numerical method developed in this paper is applied to the prediction of the groundwater flow on industrial waste landfills if we use digital color images, and the geological data, piezometric head and permeability which are gotten by the drilling survey.

Acknowledgment

We would like to thank T.Shiraishi, M. Ehara, T. Ojima, K. Saeki, H. Kato, J. Masuda, T. Kimura and M. Zhou of Koshigoe laboratory for discussions and comments on this work.

References

1. H. Fujita, H. Kawahara, H. Kawarada, Distribution theoretic approach to fictitious domain method for Neumann problems, East-West j. Numer. Mathe. 3 (2) (1995) 111-126.
2. R. Glowinski, J. L. Lions, R. Tremolieres, Numerical Analysis of Variational Inequalities, in: Studies in Mathematics and its Applications, Vol. 8, Noth-Holland, 1981.
3. H. Kawarada, Free Boundary Problem, — Theory and Numerical Method, Tokyo University Press, 1989, (in Japanese).
4. H. Koshigoe, T. Shiraishi, M. Ehara, Distribution algorithm in finite difference method and its application to a 2D simulation of temperature inversion, Journal of computational and Applied Mathematics, 232 (2009), 102-108.
5. K. Kovarik, Numerical Models in Groundwater Pollution, Springer-Verlag, 2000.
6. J.L.Lions, Perturbations Singulieres dans les Problems aux Limites et en Control Optimal, Lecture Notes in Mathematics 323, Springer-Verlag, 1973.
7. Masuda J. and Koshigoe H., Digital-finite difference method and its application to 2D simulations of flow around three circular cylinders, Technical Report of Mathematical Sciences, Chiba University, 26 [3], 2010.
8. MIC, Investigation result: Environmental dispute coordination in the Teshima Island industrial waste case (in Japanese),1995.9.
9. H. Takatsuki, The Teshima Island industrial waste case and its process towards resolution, J mater Cycles Waste Manag, 5 (2003), 26-30.
10. T. Yoshii and H. Koshigoe, A computational method for groundwater flow through industrial waste by use of digital color, Lecture Notes in Computer Science 6329,Springer, pp.288-pp.296, 2010.